Ghost-gluon coupling, power corrections, and $\Lambda_{\overline{\rm MS}}$ from lattice QCD with a dynamical charm

B. Blossier,[1] Ph. Boucaud,[1] M. Brinet,[2] F. De Soto,[3] X. Du,[2] M. Gravina,[4] V. Morenas,[5] O. Pène,[6] K. Petrov,[6] and J. Rodríguez-Quintero[7]

[1]*Laboratoire de Physique Théorique, Université de Paris XI, Bâtiment 210, 91405 Orsay Cedex;, France*
[2]*Laboratoire de Physique Subatomique et de Cosmologie, CNRS/IN2P3/UJF, 53 avenue des Martyrs, 38026 Grenoble, France*
[3]*Dpto. Sistemas Físicos, Químicos y Naturales, Univ. Pablo de Olavide, 41013 Sevilla, Spain*
[4]*Department of Physics, University of Cyprus, P.O. Box 20537, 1678 Nicosia, Cyprus, and Computation-based Science and Technology Research Center*
[5]*Laboratoire de Physique Corpusculaire, Université Blaise Pascal, CNRS/IN2P3, 63177 Aubière Cedex, France*
[6]*Laboratoire de Physique Théorique, Université de Paris XI; Bâtiment 211, 91405 Orsay Cedex; France*
[7]*Dpto. Física Aplicada, Fac. Ciencias Experimentales, Universidad de Huelva, 21071 Huelva, Spain*

(Received 2 December 2011; published 9 February 2012)

This paper is a first report on the determination of $\Lambda_{\overline{\rm MS}}$ from lattice simulations with $2+1+1$ twisted-mass dynamical flavors *via* the computation of the ghost-gluon coupling renormalized in the MOM Taylor scheme. We show this approach allows a very good control of the lattice artefacts and confirm the picture from previous works with quenched and $N_f = 2$ twisted-mass field configurations, which prove the necessity to include nonperturbative power corrections in the description of the running. We provide an estimate of $\Lambda_{\overline{\rm MS}}$ in very good agreement with experimental results. To our knowledge, it is the first calculation with a dynamical charm quark which makes the running up to $\alpha_s(M_Z)$ much safer.

DOI: 10.1103/PhysRevD.85.034503 PACS numbers: 11.15.Ha, 12.38.Aw, 12.38.Cy, 12.38.Lg

I. INTRODUCTION

QCD, the theory for the strong interactions, can be confronted with experiments only after providing it with a few inputs: one mass parameter for each quark species and the only surviving parameter in the limit of massless quarks, namely $\Lambda_{\rm QCD}$, the energy scale used as the typical boundary condition for the integration of the Renormalization Group equation for the strong coupling constant. Thus, contrary to its running that can be computed in perturbation theory, the value of the renormalized strong coupling at any scale, or equivalently $\Lambda_{\rm QCD}$, has to be taken from experiment.

The QCD running coupling can be also obtained from lattice computations, where the lattice spacing replaces $\Lambda_{\rm QCD}$ as a free parameter to be adjusted from experimental numbers: masses, decay constants, etc. Different methods have been used for the lattice calculation of $\Lambda_{\rm QCD}$. Among the most extensively applied, we can enumerate the implementation of the Schrödiger functional scheme (see, for instance, [1–4], and references therein), those based on the perturbative analysis of short-distance sensitive lattice observables as the interquark static potential (see for instance [5,6]), heavy-quark potential, Wilson loops or small Creutz ratios expanded in the ''boosted'' lattice coupling (see [7–10], and reference therein) or the vacuum polarization functions [11,12], and, in particular, those based on the study of the momentum behavior of Green functions (see [13–19], and references therein). In previous studies we compared the behavior of the 2-gluon and 3-gluon Green functions as a function of the renormalization scale with the perturbative predictions. This allowed us to get estimations for α_S and $\Lambda_{\rm QCD}$, but it also revealed the presence of nonperturbative power corrections which we interpreted as coming from the dimension-two nonzero Landau-gauge gluon condensate in an operator-product expansion (OPE) approach.[1]

In the last few years, several authors of this paper have been pursuing a program to study the running of the strong coupling, and so evaluate $\Lambda_{\rm QCD}$, grounded on the lattice determination of the ghost-gluon coupling in the so-called MOM Taylor renormalization scheme. The main advantage of this ghost-gluon approach is that the lattice computation of the coupling only involves the calculation of two-point correlators, which yields a very good control of the lattice artefacts over a large momentum window, mainly owing to the $H(4)$-extrapolation prescription [23,24], and then for a precise checking of the running. We have first analyzed the pure Yang-Mills case ($N_f = 0$) [25,26] and next extended the analysis to the case in which twisted $N_f = 2$ dynamical quarks were included in the lattice simulations [27–29]. Now, for the first time, we apply the same approach (outlined in Sec. II) to study the strong coupling by dealing with lattice simulations with two light degenerate twisted-mass flavors and a heavy doublet to include the strange and charm dynamical quarks. This is done within the framework of the European Twisted Mass (ETM) Collaboration from where we used several ensembles of gauge fields for different

[1]The possible phenomenological implications in the gauge-invariant world of such a dimension-two Landau-gauge gluon condensate and in connection with confinement scenarios has been also largely investigated, as can be seen for instance in Refs. [20,21]. This condensate has been also related to the QCD vacuum properties through the instantons liquid model [22]

bare lattice couplings, twisted masses and volume to conclude that: (i) the running description of the data requires to take into account nonperturbative power corrections, which appear to behave as OPE [30,31] predict when a nonvanishing Landau-gauge dimension-two gluon condensate is considered, and (ii) only after taking into account the nonperturbative power corrections, the lattice estimate for $\Lambda_{\rm QCD}$ strikingly agrees with the experimental result, as can be seen in Sec. IV.

II. ABOUT THE PROCEDURE

We shall follow the procedure described in detail in Refs. [25,27] to extract an estimate of $\Lambda_{\overline{\rm MS}}$ from the nonperturbative lattice determination of $\alpha_T(q^2)$, the running strong coupling renormalized in the MOM Taylor scheme and Landau gauge. Let us recall briefly how the procedure works. The Taylor coupling is defined by

$$\alpha_T(\mu^2) \equiv \frac{g_T^2(\mu^2)}{4\pi} = \lim_{\Lambda\to\infty} \frac{g_0^2(\Lambda^2)}{4\pi} G(\mu^2,\Lambda^2) F^2(\mu^2,\Lambda^2), \quad (1)$$

where F and G stand for the bare ghost and gluon dressing functions in Landau-gauge. As was thoroughly explained in Ref. [25] (see also the Appendix A of Ref. [32]), the well-known Taylor's paper [33] proved that, at any order in perturbation, the proper ghost-gluon vertex trivially takes its tree-level form when the incoming ghost momentum vanishes, this implying that the renormalization constant for this proper ghost-gluon vertex is just equal to 1 in the MOM-like scheme defined by the particular kinematics with a zero-momentum incoming ghost, i.e. Taylor scheme. This is not only true in perturbation, but it can be also concluded that taking the limit of a vanishing incoming ghost momentum drops any nonperturbative correction away from the whole proper ghost-gluon vertex, as discussed in Ref. [34]. Thus, Eq. (1) for the Landau-gauge Taylor-scheme running coupling can be straighforwardly derived from this last result.

The ghost and gluon dressing functions will be here obtained from $N_f = 2+1+1$ gauge configurations for several bare couplings, light twisted masses and volumes. Contrary to the analysis performed in Ref. [27], the interplay of light and heavy-quark mass and UV cutoff effects makes a chiral extrapolation harder. Further studies are underway for a better control of this point. Thus, for the scope of this paper, we will content ourselves with an estimation of the uncertainty due to the quark mass effects.

It should be emphasized that a crucial role is played by the appropriate elimination of discretization artefacts to provide us with reliable and exploitable results. A first step consists in curing the artefacts which are due to the breaking of the rotational invariance on the lattice, where the remaining symmetry is restricted to the $H(4)$ isometry group. For this purpose, we perform the so-called $H(4)$-extrapolation procedure [23,24,35] that leaves us with

$$\alpha_T^{\rm Latt}\left(a^2p^2, a^2\frac{p^{[4]}}{p^2}, \ldots\right) = \bar{\alpha}_T(a^2p^2) + \frac{\partial\alpha_T^{\rm Latt}}{\partial(a^2\frac{p^{[4]}}{p^2})}\Bigg|_{a^2\frac{p^{[4]}}{p^2}=0} a^2\frac{p^{[4]}}{p^2} + \ldots, \quad (2)$$

where $p^{[4]} = \sum_i p_i^4$ is the first $H(4)$-invariant (and the only one indeed relevant in our analysis). Thus, we first average over any combination of momenta being invariant under $H(4)$ ($H(4)$ orbit) and extrapolate then to the "continuum case," where the effect of $a^2p^{[4]}$ must vanish, by applying Eq. (2) for all the orbits sharing the same value of p^2, with the only assumption that the slope depends smoothly on a^2p^2 and can be fitted to a polynomial form from the whole set of lattice data. Furthermore, the $H(4)$-artefact-free lattice coupling, $\bar{\alpha}_T(a^2p^2)$ might differ from the continuum coupling by some $O(4)$-invariant artefacts, as shown, for example, in the lattice analysis of the quark-propagator renormalization constant [36–38]. This leads us finally to write

$$\bar{\alpha}_T(a^2p^2) = \alpha_T(p^2) + c_{a2p2}a^2p^2 + \mathcal{O}(a^4), \quad (3)$$

where c_{a2p2} should be fitted from the lattice data and verify the appropriate scaling from the simulations with different bare couplings β, while α_T is the lattice prediction to be compared with the continuum OPE formula for the Taylor strong coupling [27],

$$\alpha_T(\mu^2) = \alpha_T^{\rm pert}(\mu^2)\left(1 + \frac{9}{\mu^2}R(\alpha_T^{\rm pert}(\mu^2), \alpha_T^{\rm pert}(q_0^2)) \times \left(\frac{\alpha_T^{\rm pert}(\mu^2)}{\alpha_T^{\rm pert}(q_0^2)}\right)^{1-\gamma_0^{A^2}/\beta_0} \frac{g_T^2(q_0^2)\langle A^2\rangle_{R,q_0^2}}{4(N_C^2-1)}\right), \quad (4)$$

where $\gamma_0^{A^2}$ can be taken from [39,40] to give for $N_f = 4$,

$$1 - \gamma_0^{A^2}/\beta_0 = \frac{27}{132-8N_f} = \frac{27}{100}; \quad (5)$$

applying the same method outlined in the Appendix of Ref. [27], one can take advantage of the $\mathcal{O}(\alpha^4)$ computations for the Wilson coefficients in Ref. [40], and obtains

$$R(\alpha,\alpha_0) = (1 + 1.18692\alpha + 1.45026\alpha^2 + 2.44980\alpha^3) \times (1 - 0.54994\alpha_0 - 0.13349\alpha_0^2 - 0.10955\alpha_0^3), \quad (6)$$

for $q_0 = 10$ GeV. The purely perturbative running in Eq. (4) is given up to four-loops by [41]

TABLE I. Lattice setup parameters for the ensembles we used in this paper. They correspond with the ones coded as B35.48, B35.32, B55.32, and D20.48 in Table 1 of Ref. [45]. The last column stands for the number of gauge field configurations we used.

β	$\kappa_{\rm crit}$	$a\mu_l$	$a\mu_\sigma$	$a\mu_\delta$	$(L/a)^3 \times T/a$	Configurations
1.95	0.1612400	0.0035	0.135	0.170	$32^3 \times 64$	50
	0.1612400	0.0035			$48^3 \times 96$	40
	0.1612360	0.0055			$32^3 \times 64$	50
2.1	0.1563570	0.0020	0.120	0.1385	$48^3 \times 96$	40

$$\alpha_T^{\rm pert}(\mu^2)=\frac{4\pi}{\beta_0 t}\left(1-\frac{\beta_1}{\beta_0^2}\frac{\log(t)}{t}+\frac{\beta_1^2}{\beta_0^4}\frac{1}{t^2}\left(\left(\log(t)-\frac{1}{2}\right)^2+\frac{\bar\beta_2\beta_0}{\beta_1^2}-\frac{5}{4}\right)\right)+\frac{1}{(\beta_0 t)^4}\left(\frac{\bar\beta_3}{2\beta_0}+\frac{1}{2}\left(\frac{\beta_1}{\beta_0}\right)^3(-2\log^3(t)+5\log^2(t)+\left(4-6\frac{\bar\beta_2\beta_0}{\beta_1^2}\right)\log(t)-1)\right) \tag{7}$$

with $t=\ln\frac{\mu^2}{\Lambda_T^2}$ and the coefficients of the β function in Taylor scheme [25,42]. As for the $\Lambda_{\rm QCD}$ parameters in Taylor scheme and $\overline{\rm MS}$, they are related through [27]

$$\frac{\Lambda_{\overline{\rm MS}}}{\Lambda_T}=e^{-(507-40N_f/792-48N_f)}=0.560832, \tag{8}$$

for the $N_f=4$ case.[2] Thus, only three parameters, $g^2\langle A^2\rangle$, $\Lambda_{\overline{\rm MS}}$ and the coefficient for the $O(4)$-invariant artefacts c_{a2p2}, remain free to be fitted through the comparison of the prediction given by Eqs. (3) and (4) and the lattice estimate of Taylor coupling after $H(4)$ extrapolation.

III. THE LATTICE SETUP

As already mentioned, we obtain $\alpha_T^{\rm Latt}$ by Eq. (1) from the ghost and gluon propagators computed from the gauge configurations simulated at several lattices with $N_f=2+1+1$ mass-twisted lattice flavors [43] by the ETM Collaboration [44,45]. In the gauge sector, we use the Iwasaki action and compute the propagators as described in Ref. [27], while for the fermion action, we have

$$S_l=a^4\sum_x \bar\chi_l(x)(D_W[U]+m_{0,l}+i\mu_l\gamma_5\tau_3)\chi_l(x) \tag{9}$$

for the doublet of degenerate light quarks [46] and

$$S_h=a^4\sum_x \bar\chi_h(x)(D_W[U]+m_{0,h}+i\mu_\sigma\gamma_5\tau_1+\mu_\delta\tau_3)\chi_h(x) \tag{10}$$

for the heavy doublet. $D_W[U]$ is the standard massless Wilson Dirac operator. The lattice parameters for the ensembles of gauge configurations we used are given in Table I. Tuning to maximal twist is achieved by choosing a parity odd operator and determine $\kappa_{\rm crit}$ such that this operator has a vanishing expectation value. One appropriate quantity is the PCAC light-quark mass and we demand $m_{PCAC}=0$. We refer the interested reader to Refs. [44,45] for more details about the setup of the twisted-mass lattice simulations.

IV. THE RESULTS OF THE ANALYSIS

A. Curing the $H(4)$ artefacts

The first stage of the analysis, as explained above, consists in the application of the $H(4)$ extrapolation to cure the main type of discretization artefacts, namely, the ones coming from the breaking of the rotational symmetry. These effects appear to be very visible in Fig. 1(a), where we plot the ghost dressing function before and after $H(4)$ extrapolation in terms of the square of the momentum in lattice units. The classical ''fishbone'' structures generated by the different $H(4)$ orbits corresponding to the same continuum momentum can be strikingly seen before applying the extrapolation. Moreover, it is obvious that, had we rather applied some sort of average over a ''democratic'' selection of the orbits at all physical momenta, the resulting ghost dressing function would have shown an anomalously flat behavior, with no indication of the perturbative logarithm, in the large momentum region. All these anomalies appear to be strikingly cured by the $H(4)$-extrapolation prescription. It should be noted that a very important input to apply properly such a prescription comes from the many orbits at our disposal on a large momenta window (this implies to Fourier transform over large momenta). It is beneficial because, for the same price, the output is a very clean signal over a large momenta window that permits a very precise checking of the running behavior. The results of the extrapolation for the coupling in Taylor scheme are plotted against the momentum in

[2] It should be noted that, although Λ_T is gauge-dependent, $\Lambda_{\overline{\rm MS}}$ is not. Of course, the conversion factor of both parameters to each other is also gauge-dependent. Then, as far as this conversion factor can be exactly determined because of the RGE invariance of $\Lambda_{\rm QCD}$, the choice of any gauge for the lattice determination of Λ_T (Landau gauge in our case) is irrespective for the final determination of $\Lambda_{\overline{\rm MS}}$.

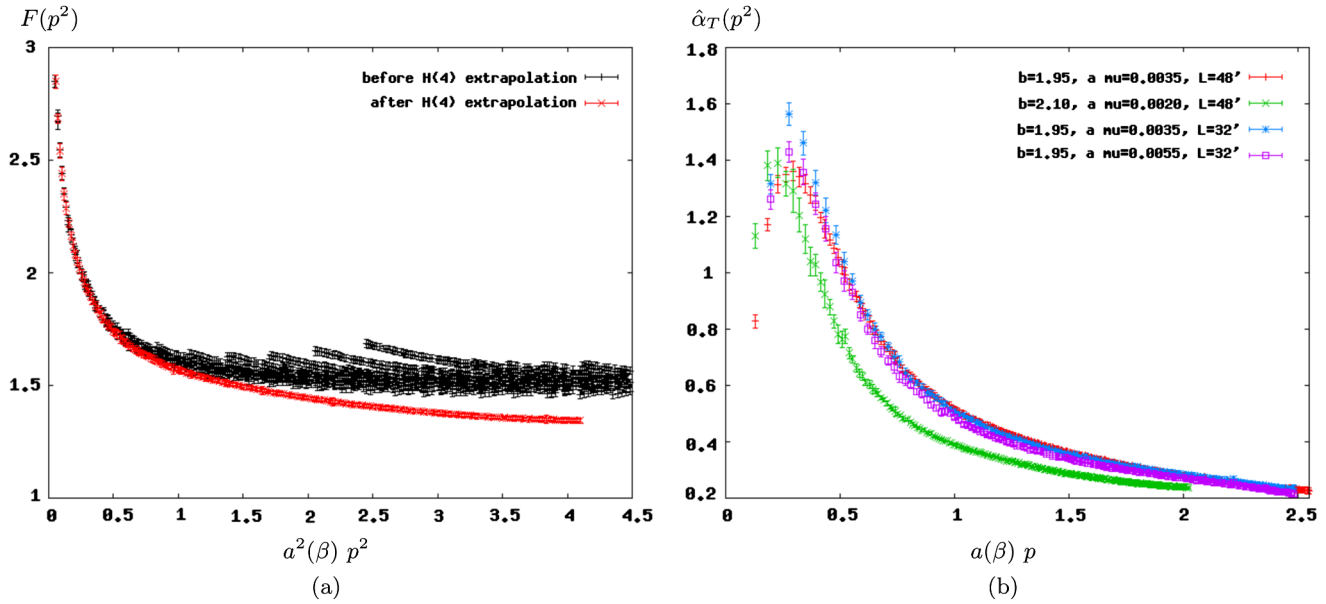

FIG. 1 (color online). (a) An example of the ghost dressing function lattice data (case: $\beta = 1.95$, $a\mu_l = 0.035$, $L = 48$) before (top black points) and after (bottom red crosses) $H(4)$ extrapolation, plotted in terms of the square of momentum in lattice units. (b) The running of the coupling as a function of the momentum in lattice units for the four ensembles of lattice data: $\beta = 1.95$ with $a\mu_l = 0.0035$ at $48^3 \times 96$ (red) and $32^3 \times 64$ lattices (blue), with $a\mu_l = 0.0055$ at $32^3 \times 64$ (violet) and $\beta = 2.1$ with $a\mu_l = 0.0020$ at $48^3 \times 96$ (green).

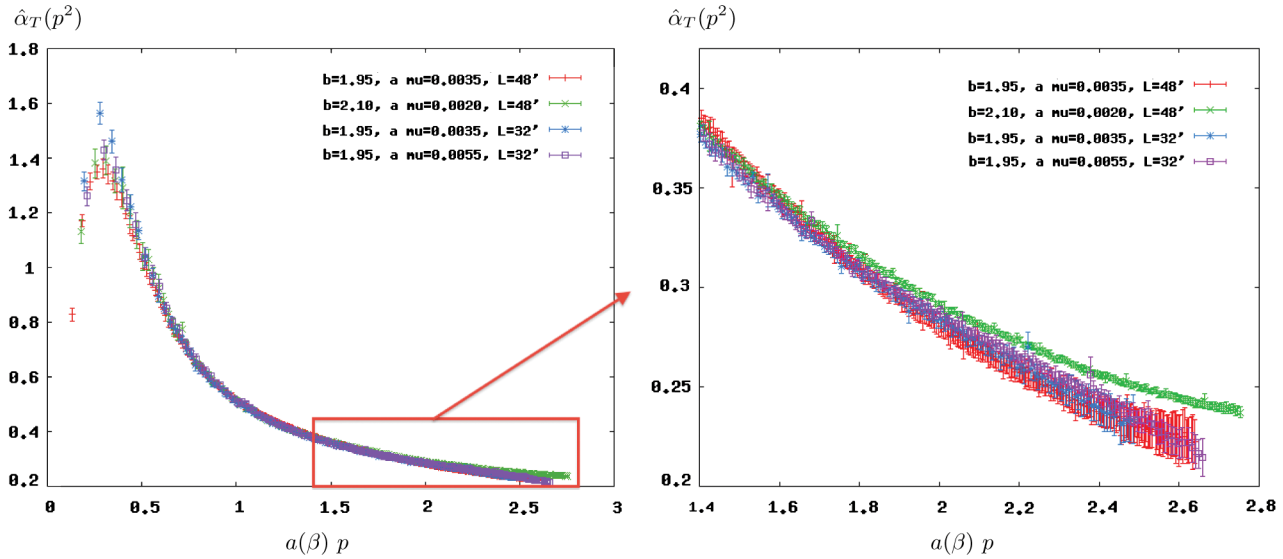

FIG. 2 (color online). The same shown in Fig. 1(b) but after the appropriate rescaling of the x axis to superimpose the four curves as much as possible. The right plot is a zoom for the large momentum region to exhibit the discrepancies indicating that $O(4)$-invariant artefacts are present.

lattice units in Fig. 1(b) for the four lattice ensembles analyzed.

B. Flavor mass, finite volume, and $O(4)$-invariant artefacts

After $H(4)$ extrapolation, a main part of the discretization artefacts are supposed to be removed and, if so, all the curves for the running coupling in Fig. 1(b) should appear superimposed after being reexpressed in terms of the momentum in physical units, at least over the momentum region where other artefacts do not play any significant role. In particular, with no further conversion, the three ones for $\beta = 1.95$ should coincide with each other (and they are close to) and the one for $\beta = 2.1$ should also after

TABLE II. Best-fit parameters for the confrontation of the different lattice data and Eqs. (3) and (4), as explained in the text. The local operator A^2 has been renormalized at $q_0 a(2.1) \simeq 3$ which corresponds to $q_0 \simeq 10$ GeV when the appropriate conversion is applied. The errors have been computed by using a jackknife procedure.

β	$a(\beta)\mu_l$	$a(\beta)\Lambda_{\overline{\rm MS}}$	$a(\beta)^2 g^2\langle A^2\rangle$	$a(\beta)/a(2.1)$	c_{a2p2}
1.95	0.0035	0.126(12)	0.7(3)	1.36(16)	−0.0047(12)
	0.0055	0.117(8)	0.57(22)	1.27(10)	
2.1	0.0020	0.092(5)	0.40(9)	1	

the appropriate rescaling of the momentum in coordinates axis. On the other hand, the comparison of the running for the three ensembles with same β parameter shows that no relevant finite volume effect happens above a lattice momentum of the order of 0.5, while a small mass effect appears to be visible: the two ensembles with same bare mass ($a\mu_l = 0.0035$) and different volumes appear nicely superimposed while the ones with same lattice volume ($32^3 \times 64$), and different bare masses seem to require an additional fine rescaling. Then, we apply a rescaling factor to the lattice momentum, when needed, to render the four curves coincident and show the results in Fig. 2. We choose to rescale all the data to those of the ensembles with $a\mu_l = 0.0035$ at $\beta = 1.95$, since their lattice spacing seems rather safely established and we have two different volumes which agree fairly well. We thus obtain an optimal rescaling factor of 1.07 for lattice momenta with $a\mu_l = 0.0055$ at $\beta = 1.95$ and a factor of 1.36 (containing both the ratio of lattice spacings and possible flavor bare mass effects) for those with $a\mu_l = 0.0020$ at $\beta = 2.1$. The agreement is indeed impressive and make us conclude that the flavor bare mass effect can be absorbed by physical calibration of the lattice spacing and be either removed by chiral extrapolation, when possible, or included in the calibration systematic uncertainty. Nevertheless, it is also manifestly shown by large lattice momentum pattern of data (see the right plot of Fig. 2) that the $O(4)$-invariant artefacts, which cannot be of course cured by the $H(4)$ extrapolation, still survive and demand some treatment for a precise analysis of the running. We will proceed to remove the remaining discretization artefacts for all our lattice data sets by applying Eq. (3) with the requirement that the coefficient c_{a2p2}, the correction being a lattice artefact, should be universal. This will be explained in the next subsection.

C. The physical running, the gluon condensate and $\Lambda_{\overline{\rm MS}}$

As explained in Sec. II, Eqs. (3) and (4) can be directly applied to fit the lattice data plotted in Fig. 1(b) with only three free parameters. In lattice units they are on one hand $\Lambda_{\overline{\rm MS}} a(\beta)$ and $g^2\langle A^2\rangle a^2(\beta)$, which depend on the lattice spacing at each simulation and on the physical values for $\Lambda_{\overline{\rm MS}}$ and for the Landau-gauge gluon condensate, and on the other hand c_{a2p2} which should be the same number for any lattice data set. In the following, we will only analyze the two ensembles at $\beta = 1.95$ simulated for $32^3 \times 64$ lattices and the one at $\beta = 2.1$ for a $48^4 \times 96$ lattice, all of them sharing approximately the same lattice volume in physical units. The ensemble at $\beta = 1.95$ for a $48^4 \times 96$ lattice, for which we exploited a smaller number of gauge configurations and have larger statistical errors, has been used to check finite-size effects. Then, as we showed that no visible finite-size effect survives above $a(\beta)p \simeq 0.5$ and that the flavor bare mass effects can be fairly well described by a lattice calibration, we fit independently any ensemble of data at both $\beta = 2.1$ and $\beta = 1.95$, by imposing the coefficient c_{a2p2} to be universal, and including a (fitted) rescaling factor to bring the heavier mass data to superimpose with the lighter ones at $\beta = 1.95$. Thus, we obtain the results of Table II for the best-fit parameters. Using these values with the appropriate rescaling, we plot in Fig. 3 the fitted running coupling obtained for the different lattices after removing all the discretization artefacts.

The universality of the coefficient c_{a2p2} and the nature of the remaining discretization artefacts that could be seen in Fig. 2 can be directly checked on the data. Actually, we have

$$\alpha_{\rm Latt}^{\beta=2.1}(a(1.95)p) - \alpha_{\rm Latt}^{\beta=1.95}(a(1.95)p) = \left(\frac{a^2(2.1)}{a^2(1.95)} - 1\right) c_{a2p2} a^2(1.95)p^2 + o(a^2(1.95)p^2), \tag{11}$$

which means that, after an appropriate rescaling implying for all the momenta to be written in units of the lattice spacing at a given reference β ($\beta = 1.95$ and $a\mu_l = 0.0035$ has been chosen here), the difference between the data for the coupling obtained at $\beta = 2.1$ and those at $\beta = 1.95$ has to be proportional to c_{a2p2} times the square of the momentum when the momentum is not too large. This is illustrated in the upper-left plot in Fig. 3, where the linear behavior on a^2p^2 is verified (for the two lighter masses). The slope given by the right-hand side (r.h.s.) of Eq. (11) with the best-fit parameters of Table II perfectly agrees with the data. In order to perform the subtraction in the left-hand side of Eq. (11) some interpolation procedure is required to estimate the values for the momenta at $\beta = 2.1$ from the data at $\beta = 1.95$. To this purpose, we used the expression given in Eqs. (3) and (4) with the best-fit parameters to analytically represent the data at $\beta = 1.95$. The result for the subtraction is shown by the black points in the plot. This procedure does not work below

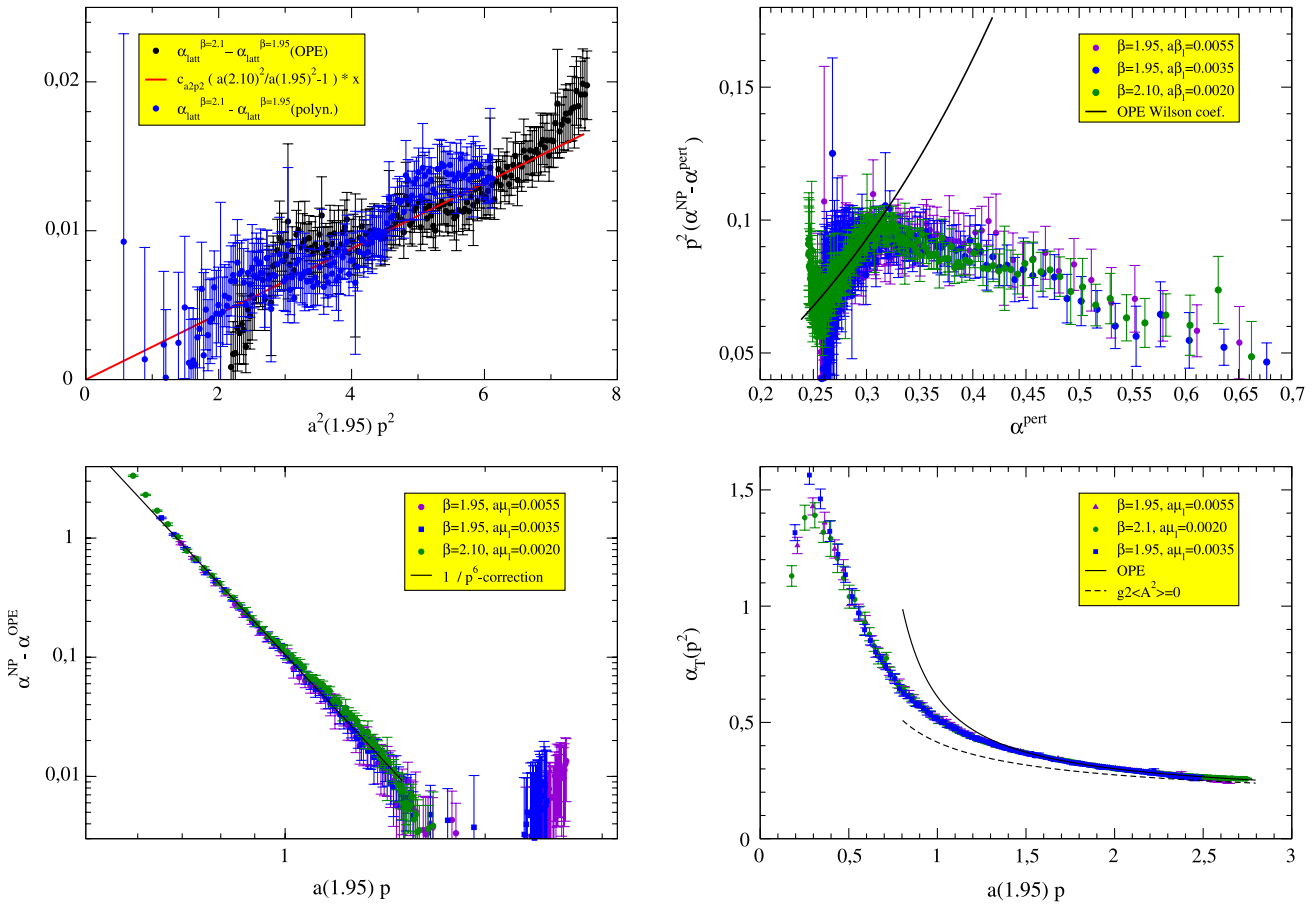

FIG. 3 (color online). (Upper-left panel) Check of Eq. (11) from the lattice data at $\beta = 1.95$ ($a\mu_l = 0.0035$) and $\beta = 2.1$ ($a\mu_l = 0.0020$), as explained in the text. (Upper-right panel) deviation from the lattice data free of discretization artefacts with respect to the prediction of the four-loop perturbative theory, with a $\Lambda_{\overline{\rm MS}}$ taken from (14), plotted in terms of the perturbative running; the solid line shows the leading nonperturbative OPE prediction, r.h.s. of Eq. (15) r.h.s. (Bottom-left panel) The departure of lattice data from the leading nonperturbative OPE prediction for the running coupling plotted in logarithmic scales, in terms of the momentum in lattice units of $a^{-1}(1.95)$: a next-to-leading $1/p^6$ behavior is strikingly manifest. (Bottom-right panel) The physical running of the strong coupling obtained from the lattice data free of discretization artefacts, expressed in terms of the momentum in units of $a^{-1}(1.95)$; the solid line stands here for the best fit with Eqs. (3) and (4), while the dotted one is for the four-loop perturbative prediction.

$a(1.95)p \simeq 1.5$, as the expressions Eqs. (3) and (4) do not represent properly the data in this region. Any other interpolating formula, as far as it fits well, would provide us with equivalent results; we illustrate this point in the plot by using also a polynomial of fourth degree to describe the lattice data at $\beta = 1.95$. The result for the subtraction in this case is given by the blue points. The only quantity we need to estimate the coefficient c_{a2p2} from the data is the ratio of lattice spacings. The large uncertainty given for these quantities in Table II is partially a consequence of our present analysis, which uses only the momentum window where the OPE prediction given by Eq. (4) appears to be in order. As far as any UV cutoff contribution should vanish at the infinite cutoff limit for the running coupling defined by Eq. (1), all the data, properly corrected for lattice artefacts, from different lattice simulations should scale when expressed in terms of physical units. Had we only then be interested in obtaining the ratio of lattice spacings, the matching would be performed over a much larger momenta window[3] and the uncertainties would be drastically reduced. Nevertheless, in the analysis of the present paper, we will follow a different fitting strategy, as will be seen in the next subsection.

D. The global fit

As we concluded in the previous subsection, the analysis of the three different lattice data sets clearly indicates that the flavor bare mass effects can be fairly well described by a lattice calibration. This means that we can suppose that

[3]One can perfom the matching all over the region where finite-size effects appear not to be visible, although the matching procedure would imply some sort of practical fit of the lattice data inside such a region. This will be the object of a forthcoming work.

the lattice spacing for any bare coupling and flavor mass can be written as

$$a(\beta,\mu_l) = a(\beta,0)(1 + c_{a\mu_l} a(\beta,0)^2 \mu_l^2 + o(a^2\mu_l^2)), \quad (12)$$

where $c_{a\mu}$ gives the slope for the chiral behavior of the lattice spacing. Of course, this light-quark bare mass dependence for the lattice spacing must be transferred to any physical quantity like the Taylor coupling, after its lattice artefacts have been removed,

$$\begin{aligned}\alpha_T(a^2(\beta,\mu_l)p^2) &= \alpha_T(a^2(\beta,0)p^2) + 2a^2(\beta,0)p^2 c_{a\mu} \\ &\quad \times \frac{d\alpha_T(x)}{dx}\bigg|_{x=a^2(\beta,0)p^2} a^2(\beta,0)\mu_l^2 + \cdots \\ &\simeq \alpha_T(a^2(\beta,0)p^2) + R_0(a^2(\beta,0)p^2)a^2(\beta,0)\mu_l^2, \quad (13)\end{aligned}$$

where we also assumed the strong coupling not to "feel" any additional light-quark bare mass effect, as it is clearly suggested by the results of the previous subsection. In the analysis of lattice configurations for $N_f = 2$ twisted-mass flavors in Ref. [27], Eq. (13) was successfully applied to extrapolate down to zero light-quark mass all the data within a narrow momentum window where R_0 in Eq. (13) was shown to be well approximated by a constant.[4] Here, we will proceed otherwise: we will take the ratios of lattice spacings, $a(\beta, a\mu_l)/a(1.95, 0.0035)$, from the previous subsection analysis and express the Taylor coupling from the three ensembles of lattice data in terms of the momentum in units of $a(1.95, 0.0035)^{-1}$. Then, we make a global fit for the three ensembles (for all momenta above $a(1.95, 0.0035)p = 1.5$) and obtain the following results:

$$\begin{aligned}\Lambda_{\overline{\rm MS}} a(1.95, 0.0035) &= 0.125(5), \\ a^2(1.95, 0.0035) g^2(q_0^2)\langle A^2\rangle_{R,q_0^2} &= 0.70(6), \quad (14) \\ c_{a2p2} &= -0.0046(7),\end{aligned}$$

with a best $\chi^2 = 103.8$ for 317 degrees of freedom. Some plots resulting from the global fit can be seen in Fig. 3.

The upper-right plot of Fig. 3 shows the lattice data, after the subtraction of the perturbative running and the $O(4)$-invariant artefacts, multiplied then by the square of the momentum in units of $a^{-1}(1.95)$ and plotted in terms of the four-loop perturbative value of the coupling at the same momentum. To obtain the perturbative coupling, we apply the value of $\Lambda_{\overline{\rm MS}}$ obtained from (14) which, after being converted to physical units with lattice spacing taken from Refs. [44,45], appears to be in very good agreement with the experimental result (see below). According to Eq. (4), one would obtain

$$\begin{aligned}p^2(\alpha_T(p^2) - \alpha_T^{\rm pert}(p^2)) &= \frac{9 g_T^2(q_0^2)\langle A^2\rangle_{R,q_0^2}}{4(N_C^2-1)} R(\alpha_T^{\rm pert}(p^2), \alpha_T^{\rm pert}(q_0^2)) \\ &\quad \times \alpha_T^{\rm pert}(q_0^2)\left(\frac{\alpha_T^{\rm pert}(p^2)}{\alpha_T^{\rm pert}(q_0^2)}\right)^{2-\gamma_0^{A^2}/\beta_0}. \quad (15)\end{aligned}$$

The solid line in the upper-right plot of Fig. 3 corresponds to the r.h.s. of Eq. (15) with the value for the Landau-gauge gluon condensate taken from Eq. (14). One should notice that the departure from zero for the lattice data in the plot can be only explained by nonperturbative contributions. Furthermore, the Wilson coefficient for the Landau-gauge gluon condensate in the OPE expansion successfully accounts for the nonflat behavior from the lattice data in the small coupling regime. This provides with a striking indication that (and where) the OPE analysis is in order. Next, in the bottom-left plot of Fig. 3, we show the departure of the lattice data from the prediction given by Eqs. (3) and (4), plotted in terms of the momentum in units of $a^{-1}(1.95)$, with logarithmic scales for both axes. The data seem to indicate that the next-to-leading nonperturbative correction is highly dominated by an $1/p^6$ term. This is just a factual statement which might suggest either that the $1/p^4$ OPE contributions are negligible when compared with the $1/p^6$ ones or that the product of the leading $1/p^4$ terms and the involved Wilson coefficients leave with an effective $1/p^6$ behavior. One might also guess that a different nonperturbative mechanism dominates over the momentum window where the dimension-four OPE condensates had to be visible. Finally, the bottom-right plot shows the physical running of the coupling and how well the OPE formula with the results from Eq. (14) fits the data.

E. Conversion to physical units

The two main purposes of this paper are to show the impact of the OPE power corrections in describing the running of the strong coupling and to give an estimate for $\Lambda_{\overline{\rm MS}}$ from lattice QCD simulations with a dynamical charm quark. The results for both goals can be summarized by the conversion to physical units for $\Lambda_{\overline{\rm MS}}$ and the Landau-gauge gluon condensate. To this purpose, we will apply

$$a(1.95, 0.0035) = \frac{a(1.95, 0.0035)}{a(1.95, 0)} a(1.95, 0), \quad (16)$$

where the absolute calibration of the lattice spacing at $\beta = 1.95$, after the chiral extrapolation for the light-quark mass, will be taken from Refs. [44,45]: $a(1.95, 0) = 0.0779(2)$ fm, and where we approximate

[4] This was found to happen for $1 \le ap \le 1.5$, where the decreasing of the derivative of α_T compensated the increasing due to the factor a^2p^2. It should be furthermore noticed that the derivative is negative, while $c_{a\mu}$ appears to be positive from the chiral extrapolation of the Sommer parameter, r_0/a, in Ref. [44]. This agrees with the sign of the chiral slope for the Taylor coupling in Ref. [27].

$$\frac{a(1.95, 0.0035)}{a(1.95, 0)} = 1^{+0.03}_{-0}. \tag{17}$$

The systematic error quoted here has been estimated from the chiral extrapolation of the Sommer parameter in Ref. [44]. There, as seen in plot 6.(b), one gets

$$\frac{(r_0/a)^{a\mu_l=0}}{(r_0/a)^{a\mu_l=0.0035}} - 1 = 0.015(11). \tag{18}$$

Then, if the string tension for the static interquark potential is supposed not to depend very much on the light-quark mass, Eq. (18) gives the conservative systematic uncertainty for the deviation from 1 in Eq. (17). Thus, we apply Eqs. (16)–(18) into Eq. (14) and obtain

$$\begin{aligned} \Lambda^{N_f=4}_{\overline{\rm MS}} &= 316 \pm 13 \pm 8^{+0}_{-9}\ \text{MeV}, \\ g^2(q_0^2)\langle A^2\rangle_{R,q_0^2} &= 4.5 \pm 0.4 \pm 0.23^{+0}_{-0.3}\ \text{GeV}^2, \end{aligned} \tag{19}$$

where the first quoted error is statistical, the second one reflects the present uncertainty on the absolute calibration of the lattice spacing that we roughly (and conservatively) estimate to be of $\pm 2.5\%$; the third one is for the chiral extrapolation of the light-quark mass. More precise estimates for these systematics uncertainties will be accessible with more data (more simulations at different β's and for more light-quark masses). Finally, the value for $\Lambda^{N_f=4}_{\overline{\rm MS}}$ and the four-loop perturbative running with the appropriate crossing of the bottom mass threshold at $m_b(m_b) = 4.19^{+18}_{-6}$ GeV [41] can be used to estimate the value of the coupling at the Z^0 mass,

$$\alpha_S(M_{Z^0}) = 0.1198(9)(5)^{+0}_{-5}, \tag{20}$$

where the errors have been properly propagated. This is a first result that will be refined, mainly by improving the precision for the estimates of systematic uncertainties. However, it appears to be pretty compatible with the last world average given by the Particle Data Group (PDG) [41]: 0.1184(7). Although a more detailed comparison of our result with PDG average and a discussion of its implications will be left for a phenomenologically targeted forthcoming letter, we should remark that our result including strange and charm dynamical quarks ($N_F = 2 + 1 + 1$) appears to be slightly larger than the lattice estimate for $N_f = 2 + 1$ staggered fermions, applied to obtain the PDG average: $\alpha_S(M_{Z^0}) = 0.1183(8)$ [10]. Assuming no systematic effect to appear from the different fermion actions, the meaning for the 1-σ discrepancy of both central values, if any, can be explained from the procedure applied to cross the threshold from $N_f = 2 + 1$ to $N_f = 2 + 1 + 1$ flavors. That procedure is very well established and controlled in perturbation theory [41,47], but some nonperturbative effects may still appear at the charm quark running mass.

Indeed, if we compare the result of $\Lambda_{\overline{\rm MS}}$ for $N_f = 2$ in Ref. [27], the central value ranging from 310 to 330 MeV (depending on the lattice size calibration at different values of β), with that for $N_f = 2 + 1 + 1$ in this paper, it can be concluded that the effect for the running coupling of crossing the strange or charm quark thresholds is not very significant[5] on $\Lambda_{\overline{\rm MS}}$. On the other hand, applying just the perturbative recipe to cross the charm quark threshold would result in a stronger decreasing of $\Lambda_{\overline{\rm MS}}$ from $N_f = 2 + 1$ to $N_f = 2 + 1 + 1$ flavors. Thus, an enhancement for the estimate of $\alpha_S(M_{Z^0})$ obtained from the $N_f = 2 + 1 + 1$ lattice result for $\Lambda_{\overline{\rm MS}}$ can be understood when comparing to the one obtained by applying that perturbative recipe to cross the charm quark threshold with the $N_f = 2 + 1$ lattice result.

V. CONCLUSIONS

We used lattice gauge field configurations with two degenerate light and one heavy doublet of twisted-mass flavors, produced within the framework of ETM Collaboration, to compute the running strong coupling in the MOM Taylor scheme. In this particular renormalization scheme, the lattice computation of this coupling has the very nice feature of involving only propagators. This allows for a very precise control of the lattice artefacts and other systematic uncertainties. In particular, the so-called $H(4)$-extrapolation procedure, which has already been proven very effective at eliminating the discretization artefacts of two-point correlation functions, is efficiently at work in this analysis. The dominant $O(4)$ artefact is also rather easily isolated and eliminated. On the other hand, the renormalized coupling, defined in the MOM Taylor scheme by the combination of the ghost and gluon bare propagators, must only depend on the UV cutoff through residual contributions vanishing at the infinite cutoff limit. Thus, the Taylor coupling computed from the lattice must join the continuum prediction at this infinite cutoff limit. This is also a strong point to cure properly lattice artefacts and get reliable results. Thus, we evaluated the running strong coupling over a rather large window of lattice momenta and, after the appropriate relative calibration, confront it with the perturbative prediction available at the four-loop level. We clearly demonstrate the necessity to include nonperturbative power corrections to get an accurate description for the behavior of the coupling

[5]In Sec. 4.5 of Ref. [27], a significant difference between quenched ($N_f = 0$) and $N_f = 2$ lattice results for $\Lambda_{\overline{\rm MS}}$ (once lattice spacing is calibrated from f_π) was observed. In that case, simulations for infinite (quenching) and vanishing (chiral limit) quark flavors were compared, although it is well-known that the chiral lmit for the quenched case is wrong. On the contrary, when comparing $N_f = 2 + 1 + 1$ and $N_f = 2$ (or $N_f = 2 + 1$) cases, we deal with infinitely massive flavors (s and c) in the latter and heavy (c) or midheavy (s) in the former. Then, not to see the same significant effect cannot be too surprising.

constant. We then show these corrections follow the OPE predictions when a nonvanishing dimension-two Landau-gauge gluon condensate is present. This is to our knowledge the first time a Wilson coefficient is directly confronted to numerical results. Higher order terms are visible and seem to be dominated by $1/p^6$ contributions instead of the expected $1/p^4$ ones.

The precise comparison of lattice estimates with continuum formula allows the estimate of both the gluon condensate and $\Lambda_{\overline{\rm MS}}$. The latter is in a very good agreement with the world average of its experimental determinations provided by PDG, confirming that the picture we advanced, first by the analysis of quenched lattice data and next by studying lattice simulations with two twisted-mass flavors, agrees very well with the real world when a full QCD analysis is performed including a heavy doublet for strange and charm quarks. Going the other way around, with the experimental value for $\Lambda_{\overline{\rm MS}}$ as an input, this approach could be used to provide quite good absolute determinations of the lattice spacings. Relative measurements (ratio of lattice spacings) through the superimposition of the different curves for $\alpha(a^2p^2)$ over a large window can be also obtained with a good level of precision. The perturbative running from our results up to the Z boson mass is well-known in perturbation theory and we apply the standard formula [41] to cross the b quark threshold. We do not need to consider the charm quark threshold since, for the first time to our knowledge, we have used dynamical charm in our computation. This is a very significant gain: the crossing of the charm threshold using perturbative QCD is quite questionable, since, as we have seen, nonperturbative effects (OPE power terms) are sizeable at this energy.

Further works are in progress. In particular data with different masses at $N_f = 2 + 1 + 1$ and from simulations with $N_f = 4$ light flavors will soon be available to help to improve on the question of the mass effect.

ACKNOWLEDGMENTS

We are particularly indebted to A. Le Yaouanc, J. P. Leroy, and J. Micheli for participating in many fruitful discussions at the preliminary stages of this work and to S. F. Reker and G. C. Rossi for their very attentive reading of the manuscript and valuable comments. We also thank the IN2P3 Computing Center (CNRS-Lyon), the apeNEXT computing laboratory (Rome), and the computing center at IDRIS (CNRS-Orsay) for provinding numerical resources. J. R.-Q. is indebted to the Spanish MICINN for the support from research Project No. FPA2009-10773 and to "Junta de Andalucia" from Project No. P07FQM02962.

[1] M. Luscher, R. Sommer, P. Weisz, and U. Wolff, Nucl. Phys. **B413**, 481 (1994).
[2] G. M. de Divitiis, R. Frezzotti, M. Guagnelli, and R. Petronzio, Nucl. Phys. **B433**, 390 (1995).
[3] M. Della Morte *et al.* (ALPHA), Nucl. Phys. **B713**, 378 (2005).
[4] S. Aoki *et al.* (PACS-CS), J. High Energy Phys. 10 (2009) 053.
[5] S. Booth *et al.* (UKQCD Collaboration), Phys. Lett. B **294**, 385 (1992).
[6] N. Brambilla, X. Garcia i Tormo, J. Soto, and A. Vairo, Phys. Rev. Lett. **105**, 212001 (2010).
[7] M. Gockeler *et al.*, Phys. Rev. D **73**, 014513 (2006).
[8] Q. Mason *et al.* (HPQCD), Phys. Rev. Lett. **95**, 052002 (2005).
[9] K. Maltman, D. Leinweber, P. Moran, and A. Sternbeck, Phys. Rev. D **78**, 114504 (2008).
[10] C. Davies *et al.* (HPQCD Collaboration), Phys. Rev. D **78**, 114507 (2008).
[11] E. Shintani *et al.*, Proc. Sci., LAT2009 (2009) 207.
[12] E. Shintani, S. Aoki, H. Fukaya, S. Hashimoto, T. Kaneko *et al.*, Phys. Rev. D **82**, 074505 (2010).
[13] B. Alles, D. Henty, H. Panagopoulos, C. Parrinello, C. Pittori *et al.*, Nucl. Phys. **B502**, 325 (1997).
[14] P. Boucaud, J. Leroy, J. Micheli, O. Pène, and C. Roiesnel, J. High Energy Phys. 10 (1998) 017.
[15] P. Boucaud *et al.*, J. High Energy Phys. 04 (2000) 006.
[16] P. Boucaud, A. Le Yaouanc, J. Leroy, J. Micheli, O. Pène, and J. Rodríguez-Quintero, Phys. Lett. B **493**, 315 (2000).
[17] P. Boucaud, A. Le Yaouanc, J. Leroy, J. Micheli, O. Pène, and J. Rodríguez-Quintero, Phys. Rev. D **63**, 114003 (2001).
[18] P. Boucaud *et al.*, J. High Energy Phys. 01 (2002) 046.
[19] A. Sternbeck *et al.*, Proc. Sci., LAT2007 (2007) 256.
[20] F. V. Gubarev and V. I. Zakharov, Phys. Lett. B **501**, 28 (2001).
[21] D. Dudal, R. Sobreiro, S. Sorella, and H. Verschelde, Phys. Rev. D **72**, 014016 (2005).
[22] P. Boucaud *et al.*, Phys. Rev. D **66**, 034504 (2002).
[23] D. Becirevic, P. Boucaud, J. Leroy, J. Micheli, O. Pene, J. Rodriguez-Quintero, and C. Roiesnel, Phys. Rev. D **60**, 094509 (1999).
[24] F. de Soto and C. Roiesnel, J. High Energy Phys. 09 (2007) 007.
[25] P. Boucaud, F. De Soto, J. Leroy, A. Le Yaouanc, J. Micheli, O. Pène, and J. Rodríguez-Quintero, Phys. Rev. D **79**, 014508 (2009).
[26] J. Rodriguez-Quintero *et al.*, Proc. Sci., QCD-TNT09 (2009) 039.
[27] B. Blossier *et al.* (ETM), Phys. Rev. D **82**, 034510 (2010).
[28] B. Blossier *et al.* (ETM), Proc. Sci., LATTICE2010 (2010) 227.

[29] O. Pène, B. Blossier, P. Boucaud, A. Yaouanc, J. Leroy *et al.*, Proc. Sci., FACESQCD (2011) 010.
[30] M. A. Shifman, A. Vainshtein, and V. I. Zakharov, Nucl. Phys. **B147**, 385 (1979).
[31] M. A. Shifman, A. Vainshtein, and V. I. Zakharov, Nucl. Phys. **B147**, 448 (1979).
[32] P. Boucaud, J. Leroy, A. Yaouanc, J. Micheli, O. Pene *et al.* Few-Body Syst. (2011).
[33] J. Taylor, Nucl. Phys. **B33**, 436 (1971).
[34] P. Boucaud, D. Dudal, J. Leroy, O. Pene, and J. Rodriguez-Quintero, J. High Energy Phys. 12 (2011) 018.
[35] D. Becirevic, P. Boucaud, J. Leroy, J. Micheli, O. Pene, J. Rodriguez-Quintero, and C. Roiesnel, Phys. Rev. D **61**, 114508 (2000).
[36] P. Boucaud, F. de Soto, J. Leroy, A. Le Yaouanc, J. Micheli *et al.*, Phys. Lett. B **575**, 256 (2003).
[37] P. Boucaud, F. de Soto, J. Leroy, A. Le Yaouanc, J. Micheli *et al.*, Phys. Rev. D **74**, 034505 (2006).
[38] B. Blossier *et al.*, Phys. Rev. D **83**, 074506 (2011).
[39] J. A. Gracey, Phys. Lett. B **552**, 101 (2003).
[40] K. Chetyrkin and A. Maier, J. High Energy Phys. 01 (2010) 092.
[41] K. Nakamura *et al.* (Particle Data Group), J. Phys. G **37**, 075021 (2010).
[42] K. Chetyrkin and A. Retey, arXiv:hep-ph/0007088.
[43] R. Frezzotti, P. A. Grassi, S. Sint, and P. Weisz (Alpha), J. High Energy Phys. 08 (2001) 058.
[44] R. Baron, P. Boucaud, J. Carbonell, A. Deuzeman, V. Drach *et al.* (ETM Collaboration), J. High Energy Phys. 06 (2010) 111.
[45] R. Baron, B. Blossier, P. Boucaud, J. Carbonell, A. Deuzeman *et al.* (ETM Collaboration), Proc. Sci., LATTICE2010 (2010) 123.
[46] R. Frezzotti and G. C. Rossi, Nucl. Phys. B, Proc. Suppl. **128**, 193 (2004).
[47] K. Chetyrkin, J. H. Kuhn, and C. Sturm, Nucl. Phys. **B744**, 121 (2006).